Physica E: Low-dimensional Systems and Nanostructures 105 (2019) 83–89

Contents lists available at ScienceDirect

Physica E: Low-dimensional Systems and Nanostructures

journal homepage: www.elsevier.com/locate/physe

Magnetic field effect on nonlocal resonance frequencies of structure-based filter with periodic square holes network

Rachid Kerid[a,*], Hicham Bourouina[b], Réda Yahiaoui[c], Mhamed Bounekhla[a], Abdelkader Aissat[d]

[a] LabSET, Institute of Electronics, University of Blida, BP. 270 09000, Algeria
[b] Laboratoire de physique, Ecole Normale Supérieure Bou-Saada, 28200 M'Sila, Algeria
[c] Institute FEMTO-ST, Université de Franche-Comté, CNRS, F-25044 Besancon, Cedex, France
[d] LASICOM Laboratory, Faculty of the Engineering Sciences, University Saad Dahlab Blida, Algeria

ARTICLE INFO

Keywords:
Magnetic field
Periodic square holes
Resonance frequency
Equivalent parameters
Nonlocal elasticity

ABSTRACT

In this paper, we investigate the magnetic field, thermal loads and small scale effects on the dynamics vibration of a nanobeam structure composed of a rectangular configuration perforated with periodic square holes network and subjected to axial magnetic field based on Euler–Bernoulli beam model (EBM) and Timoshenko beam model (TBM). The developed resonance frequencies expressions are derived by modifying the standard equations of dynamics beam vibration. The small scale effect is adopted via the Eringen's nonlocal theory while the coupled governing equations are obtained and solved using analytical solution method in order to determine the resonance frequency of perforated nanobeam. It is found that the resonance frequency change, the magnetic field intensity, the thermal loads and small scale effects are in dependence with geometrical parameters such as size and number of holes. Therefore, these results are discussed for the investigation of the structure dynamic deformation and compared with literature results where new remarks are deduced and presented with detail for a proper design of M/NEMS structures.

1. Introduction

In recent years, the contribution of interaction and coupling effects between mechanical, electric and magnetic fields is a novel candidate for the study of the dynamic vibration and buckling behavior of nanobeam based on the Eringen's nonlocal elasticity theory, which takes into account the small scale effect and the Timoshenko beam theory which relates the bending moment, rotary inertia and shear forces have interested many researchers [1–5], whereas, Maxwell equations for electrostatics and magnetostatics are used to model of the electric and magnetic behavior. Analytical models of the beam are derived by modifying the standard Timoshenko beam equations for static deflection, buckling and vibration behavior. Therefore, several experimental and theoretical studies are carried out in order to investigate the dynamic behavior of nanostructures integrated in micro/nano-electromechanical systems (M/NEMS) such as nanowires [6–9], nanoplates [10] and carbon nanotubes [11–14].

Nevertheless, to investigate the magnetic field, small scale and thermal loads effects in nanoscale structures in which the interatomic bonds play a vital role on their deflection, several authors have introduced different approaches and proposed to use additional parameters such as of surface stress [15], piezoelectric parameters [16], thermal loads, electrical and magnetic force [17–24]. These contributions are providing the basis for new ways of analysis that the resonance frequency change with nanobeam size, shape and additional effect conditions.

Nowadays, perforation is a geometric procedure widely used in advanced technologies to develop sensitive structures especially for optomechanics and photonics [25,26]. Despite the crucial role of perforation in the current technologies, the perforated nanostructures behavior has not been analyzed as extensively as full nanostructures behavior but only for particular cases due to the problem complication. Sharpe et al. [27] investigated the holes size effect on the mechanical characteristics of polysilicon thin film, and they confirmed that the Young's modulus value decrease of 12% and the strength of the holed specimens drops by 50%. Rabinovich et al. [28] investigated the holes size effect on Young's modulus and shear modulus by studying the electromechanical behavior of a perforated beam structure. Their results showed that Young's modulus and shear modulus are directly affected by holes size with a decrease of 24% and 30% respectively.

* Corresponding author.
E-mail addresses: r.kerid@ensh.dz (R. Kerid), hi.bourouina@gmail.com (H. Bourouina), reda.yahiaoui@femto-st.fr (R. Yahiaoui), bounekhla.mhamed@yahoo.fr (M. Bounekhla), sakre23@yahoo.fr (A. Aissat).

https://doi.org/10.1016/j.physe.2018.05.021
Received 25 November 2017; Received in revised form 6 May 2018; Accepted 18 May 2018
Available online 19 May 2018
1386-9477/

Besides, the effect of holes in the resonance frequencies for perforated beams which may be considered as a significant parameter in which *Luschi* and *Pieri* [29,30] have developed analytical expressions for the equivalent bending stiffness and shear stiffness for perforated beam structures with periodic square holes network, and they have determined the resonance frequencies expression. According to the literature, dynamic behavior of size-dependent perforated nanobeams subjected to axial magnetic field is a novel topic that has not been reported.

In this work, numerical results are given to demonstrate the influence of magnetic field, small scale and thermal loading effects on the resonance frequency of a perforated nanobeam for varying numbers and sizes of holes using an analytical model of this structure. The paper is organized as follows: in section 2, theoretical formulation and geometrical structure for perforated nanobeam subjected to Lorentz force induced by the applied axial magnetic field is presented. In section 3, new resonance frequency model based on nonlocal elasticity and Timoshenko beam theories is developed. In section 4, the magnetic field, small scale and thermal loading effects are investigated on the free dynamics vibration with numerical calculations and detailed discussions. Concluding remarks of work are given in section 5.

2. Problem formulation

2.1. Structure geometry description

The dynamics vibration of perforated nanobeam subjected to magnetic field and thermal loading in this study will be analyzed via the Eringen's nonlocal theory and the Timoshenko beam theory with the equivalent parameters for bending and shear stiffness developed by *Luschi* and *Pieri* [29]. In so doing, we consider a nanobeam of length L, width b and thickness h, with periodic square holes network of spatial period s_P and size of hole d_h, we can also defined N as the number of holes distributed along the section, and $\beta = (d_h/s_P)$ as the hole size ratio which can range from 0 (full beam) to 1. Fig. 1 presents the geometrical structure under consideration.

2.2. Maxwell's relations

We consider the Lorentz force f_{LZ} induced by a static, uniform, longitudinal, external magnetic field to the nanobeam in the z direction. According to the following equations, we can define, the static charge density (ρ_b), current density vector (J), electric vector (E), magnetic field intensity (H), magnetic field density (B) and displacement current density (D) as described in Ref. [23]. However, Maxwell equations can be divided in three groups as follow:

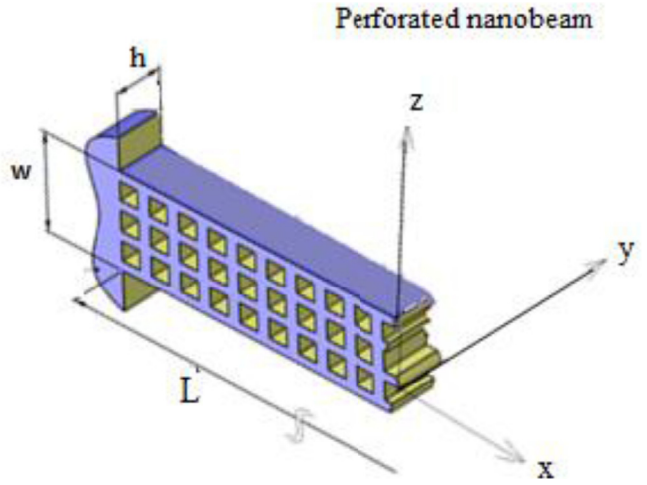

Fig. 1. Geometry and coordinates of perforated nanobeam structure with periodic square holes network. Part of the full-length of structure is cut away for more clarification.

- Equations of electromagnetic coupling.

$$\nabla \times H = J + \frac{\partial D}{\partial t}$$
$$\nabla \times E = -\frac{\partial B}{\partial t} \quad \text{(Generalized Ampere theorem and the Lenz} - \text{Faraday Law)} \tag{1}$$

- Equations of conservation.

$$\nabla \cdot B = 0$$
$$\nabla \cdot J = 0$$
$$\nabla \cdot D = \rho \tag{2}$$

- Equations of property of materials and environment.

$$B = \eta H + B_r$$
$$D = \varepsilon E$$
$$J = \sigma\left(E + \frac{\partial U}{\partial t} \times B\right) \tag{3}$$

Where Br is remanent induction of the material (for the first magnetization with no applied field H, the Br field is zero), ε and η are the electric and magnetic permeability of the nanobeam, respectively, and if we consider the nanobeam have a global isotropy, these two parameters are supposed scalar. Also, with neglecting the displacement of current density D and its derivative with respect to time, the electromagnetic field can be expressed by:

$$E = E_0 + e,$$
$$H = H_0 + h \tag{4}$$

Where $e = (x, y, z, t)$ and $h = (x, y, z, t)$ are the small disturbances of the primary applied electromagnetic field quantities, E_0 and H_0, respectively, in which $E_0 = 0$, thus, $E = e$. So, under these assumptions, Maxwell's equations can be written in the following form:

$$J = \nabla \times h, \quad \nabla \times e = -\eta \frac{\partial h}{\partial t} \tag{5}$$

$$\nabla h = 0, \quad e = -\eta\left(\frac{\partial u}{\partial t} \times H_0\right) \tag{6}$$

$$h = \nabla \times (u \times H_0) \tag{7}$$

In which $\boldsymbol{u}$ is the displacement field vector $\boldsymbol{u} = (u, 0, w)$ of nanobeam. Considering the axial magnetic field $H = (H_x, 0, 0)$ as a vector acting on the perforated nanobeam, we can write that:

$$h = -H_x\left(\frac{\partial v}{\partial y} + \frac{\partial w}{\partial z}\right)i + H_x\frac{\partial v}{\partial x}j + H_x\frac{\partial w}{\partial x}k \tag{8}$$

The Lorentz force induced by the applied axial magnetic field is obtained as

$$f = f_x i + f_y j + f_z k = \eta(J \times H)$$
$$= \eta\left[0i + H_x^2\left(\frac{\partial^2 v}{\partial x^2} + \frac{\partial^2 v}{\partial y^2} + \frac{\partial^2 w}{\partial y \partial z}\right)j + H_x^2\left(\frac{\partial^2 w}{\partial x^2} + \frac{\partial^2 w}{\partial y^2} + \frac{\partial^2 v}{\partial y \partial z}\right)k\right] \tag{9}$$

In this study, we consider the displacement of nanobeam $w(x,t)$ and the Lorentz force act only in the z direction, therefore, the resultant Lorentz force in the transverse direction is written as [23]:

$$f_{LZ} = \eta \int_A f_Z \, dA = \eta A_{eq} H_x^2 \frac{\partial^2 w}{\partial x^2} \tag{10}$$

3. Mathematical model

3.1. Governing motion equation

On the basis of the Euler–Bernoulli beam theory which takes into account the effect bending stiffness and Timoshenko beam theory which included the shear effect as well as the rotation effect, in addition to the bending effect. The bending moment M and the shear force V can be given by nonlocal expressions with the nonlocal coefficient proposed by Eringen in Ref. [32]. Therefore, the nonlocal bending moment M and the nonlocal shear force V as function of the flexural deflection w and the rotation angle ψ of the area cross-section are given by Equations (11) and (12).

$$M = \mu^2\frac{\partial^2 M}{\partial x^2} + EI_{eq}\frac{\partial \psi}{\partial x} \tag{11}$$

$$V = \mu^2\frac{\partial^2 V}{\partial x^2} + kAG_{eq}\left(\frac{\partial w}{\partial x} - \psi\right) \tag{12}$$

where EI_{eq} is the equivalent bending stiffness, GA_{eq} is the equivalent shear stiffness, the coefficient k is the shear factor equal 5/6 for a rectangular cross-section [22] and μ is the nonlocal parameter characterizing the small-scale effect which is estimated by *Yang* and *Lim* [41] as $\mu = \mu^* L$ with $\mu^*\varepsilon[0,0.2]$.

The standard Timoshenko equations for the dynamic vibration of a perforated nanobeam subjected to a magnetic field can be described by two coupled differential equations given in terms of the flexural deflection w and the rotation angle ψ of the cross-section. Thus the coupled equations have been written as [3,31–33]

$$\frac{\partial V}{\partial x} - \rho A_{eq}\frac{\partial^2 w}{\partial t^2} + F_R\frac{\partial^2 w}{\partial x^2} = 0 \tag{13}$$

$$\frac{\partial M}{\partial x} + V = \rho I_{eq}\frac{\partial^2 \psi}{\partial t^2} \tag{14}$$

where ρA_{eq} is the equivalent mass per unit length and ρI_{eq} is the equivalent rotational inertia per unit length. $F_R = F_t - F_{LZ}$ is the result of Lorentz force induced by the axial magnetic force given in Equation (10) and the axial thermal force which is related to the temperature change T and the thermal expansion parameter of the beam material θ [25,45,46].

$$F_t = \left(\frac{EI_{eq}\rho A_{eq}}{\rho I_{eq}}\right)\theta T \tag{15}$$

By substituting Equations (11) and (12) into (13) and (14) gives the nonlocal bending moment M and the nonlocal shear force V as:

$$M = (EI_{eq})\frac{\partial \psi}{\partial x} + \mu^2\left[\rho I_{eq}\frac{\partial^3 \psi}{\partial x \partial t^2} - (\rho A_{eq})\frac{\partial^2 w}{\partial t^2} + F_R\frac{\partial^2 w}{\partial x^2}\right] \tag{16}$$

$$V = kAG_{eq}\left(\frac{\partial w}{\partial x} - \psi\right) + \mu^2\left[(\rho A_{eq})\frac{\partial^3 w}{\partial x \partial t^2} - F_R\frac{\partial^3 w}{\partial x^3}\right] \tag{17}$$

Now, by inserting Equations (16) and (17) into (11) and (12) respectively, the nonlocal explicit version of the coupled dynamic equations for a Timoshenko perforated nanobeam with magnetic field, small scale and thermal loads effects can be obtained as:

$$kAG\frac{\partial}{\partial x}\left[\frac{\partial w}{\partial x} - \psi\right] + F_R\frac{\partial^2}{\partial x^2}\left[w - \mu^2\frac{\partial^2 w}{\partial x^2}\right] = (\rho A_{eq})\frac{\partial^2}{\partial t^2}\left[w - \mu^2\frac{\partial^2 w}{\partial x^2}\right] \tag{18}$$

$$EI_{eq}\frac{\partial^2 \psi}{\partial x^2} + kAG_{eq}\left(\frac{\partial w}{\partial x} - \psi\right) = \rho I_{eq}\frac{\partial^2}{\partial t^2}\left[\psi - \mu^2\frac{\partial^2 \psi}{\partial x^2}\right] \tag{19}$$

By differentiating Equation (18) with respect to x and replacing the term $\partial\psi/\partial x$ from Equation (19), the nonlocal differential equation via Timoshenko beam theory obtained is:

$$\begin{aligned}
&\frac{1}{\rho A_{eq}}\left(EI_{eq} + \mu^2 F_R + \frac{F_R EI_{eq}}{kGA_{eq}}\right)\frac{\partial^4 w}{\partial x^4} - \frac{F_R}{\rho A_{eq}}\frac{\partial^2 w}{\partial x^2} \\
&- \left(\frac{F_R}{\rho A_{eq}}\frac{\rho I_{eq}}{kGA_{eq}} + \frac{EI_{eq}}{kGA_{eq}} + \frac{\rho I_{eq}}{\rho A_{eq}} + \mu^2\right)\frac{\partial^4 w}{\partial x^2 \partial t^2} + \frac{\rho I_{eq}}{kGA_{eq}}\frac{\partial^4 w}{\partial t^4} \\
&- \left(\mu^4\frac{F_R}{\rho A_{eq}}\frac{\rho I_{eq}}{kGA_{eq}}\right)\frac{\partial^8 w}{\partial x^6 \partial t^2} \\
&+ \mu^4\frac{\rho I_{eq}}{kGA_{eq}}\frac{\partial^8 w}{\partial x^4 \partial t^4} - \mu^2\frac{F_R}{\rho A_{eq}}\frac{EI_{eq}}{kGA_{eq}}\frac{\partial^6 w}{\partial x^6} + \left[\mu^2\left(\frac{\rho I_{eq}}{\rho A_{eq}} + 2\frac{F_R}{\rho A_{eq}}\frac{\rho I_{eq}}{kGA_{eq}}\right)\right. \\
&\left. + \frac{EI_{eq}}{kGA_{eq}}\right]\frac{\partial^6 w}{\partial x^4 \partial t^2} - 2\mu^2\frac{\rho I_{eq}}{kGA_{eq}}\frac{\partial^6 w}{\partial x^2 \partial t^4} + \frac{\partial^2 w}{\partial t^2} = 0
\end{aligned} \tag{20}$$

Besides that, *Luschi* and *Pieri* [29] found the analytical expressions for the equivalent parameters ρA_{eq}, ρI_{eq}, EI_{eq} and GA_{eq} as functions of the number of holes N and the filling ratio $\alpha = (1-\beta)$. The analytical expressions of ρA_{eq}, ρI_{eq}, EI_{eq}, GA_{eq} ρ_{eq} *and* A_{eq}, have been calculated by using equations (21)–(26) respectively.

$$EI_{eq} = \frac{EI_{eb}(N+1)\alpha(N^2+2N+\alpha^2)}{(1-\alpha^2+\alpha^3)N^3 + 3\alpha N^2 + (3+2\alpha-3\alpha^2+\alpha^3)\alpha^2 N + \alpha^3} \tag{21}$$

$$\rho A_{eq} = \rho A_{eq}\frac{(1-N(\alpha-2))\alpha}{N+\alpha} \tag{22}$$

$$AG_{eq} = A\frac{N+1}{N}\frac{E}{2}\alpha^2 \tag{23}$$

$$\rho I_{eq} = \rho I_{eb}\frac{\alpha((2-\alpha)N^3 + 3N^2 - 2(\alpha-3)(\alpha^2-\alpha+1)N + \alpha^2 + 1)}{(N+\alpha)^3} \tag{24}$$

$$\rho_{eq} = \alpha(2-\alpha)\rho \tag{25}$$

According to Equations (22) and (25) the term A_{eq} formulated as follow:

$$A_{eq} = A\frac{[1-N(\alpha-2)]}{(N+\alpha)(2-\alpha)} \tag{26}$$

where E is the Young's modulus, ρ is the density of material, I and A are respectively, the moment of inertia and the area of nanobeam's cross section corresponding to a full beam.

3.2. Nonlocal resonance frequency

The solution of governing equations of simply-supported nanobeam with the flexural deflection can be given by the following form [25,41–44].

$$w(x,t) = \overline{W}\sin(\lambda_n x)\cos(\lambda_n t) \tag{27}$$

where ω is the angular frequency, $\overline{W}$ is maximum flexural deflection and $\lambda_n = n\pi/L$ is the wave number of vibration.

Thus, the nonlocal resonance frequencies via Timoshenko beam model (TBM) obtained with new formulation as:

$$(\omega_n^2)_{NT} = \frac{a}{2b}\left[1 \pm \sqrt{1 - \frac{4bc}{a^2}}\right] \tag{28}$$

Where a, b and c are given by:

$$\begin{aligned}
a = &\left(1 + \frac{F_R}{\rho A_{eq}}\frac{\rho I_{eq}}{kGA_{eq}} + \frac{EI_{eq}}{kGA_{eq}} + \frac{\rho I_{eq}}{\rho A_{eq}} + \mu^2\right)\lambda^2 + \mu^4\frac{F_R}{\rho A_{eq}}\frac{\rho I_{eq}}{kGA}\lambda^6 \\
&+ \mu^2\left[\left(\frac{\rho I_{eq}}{\rho A_{eq}} - 2\frac{F_R}{\rho A_{eq}}\frac{\rho I_{eq}}{kGA_{eq}}\right) + \frac{EI_{eq}}{kGA_{eq}}\right]\lambda^4
\end{aligned} \tag{29}$$

$$b = \frac{\rho I_{eq}}{kGA_{eq}}(1 + \mu^4\lambda^4 + 2\mu^2\lambda^2) \tag{30}$$

$$c = \frac{1}{\rho A_{eq}}\left[\left(EI_{eq} + \mu^2 F_R + F_R\frac{EI_{eq}}{kGA_{eq}}\right)\lambda^4 + F_R\lambda^2 + \mu^2 F_R\lambda^6\right] \tag{31}$$

When the rotary inertia and shear distortion effects are ignored, equation (20) is reduced to the governing equation of Euler-Bernoulli beam model (EBM) under axial magnetic field with small scale effects as follows [29,34,36,37,40]:

$$EI_{eq}\frac{\partial^4 w}{\partial x^4} + \rho A_{eq}\frac{\partial^2 w}{\partial t^2} - F_R\frac{\partial^2 w}{\partial x^2} - \mu^2\left(\rho A_{eq}\frac{\partial^4 w}{\partial x^2 \partial t^2} - F_R\frac{\partial^4 w}{\partial x^4}\right) = 0 \quad (32)$$

According to the existence condition of nonzero solution $w_{\max}$ of equation (27), the resonance frequency based on nonlocal EBM model is obtained as follows:

$$(\omega_n^2)_{NE} = \frac{EI_{eq}\lambda_n^4}{\rho A_{eq}(1+\mu^2\lambda_n^2)} + \frac{F_R\lambda_n^2}{\rho A_{eq}} \quad (33)$$

4. Results and discussions

This section devotes to investigate the magnetic field, small scale, thermal loads effects on the resonance frequencies on the basis of the above formulation of a simply-supported perforated nanobeam with length $L = 100$ nm, width $b = L/10$ and thickness $h = b/2$. The Young's modulus of material is a key parameter used in NEMS, which is selected as single crystal silicon such that $E = 169$ GPa, density $\rho = 2330$ kg/m^3 [29]. The permeability of magnetic field is considered to be $4\pi 10^{-7}$, thermal expansion coefficient $\theta = 2.57.10^{-6}K^{-1}$, $B = 15.8$ MPa/K and $T_0 = 317$ K, Thus, we have employed the equivalent parameters values EI_{eq}, GA_{eq}, ρA_{eq} and ρI_{eq} which are calculated as a function of number of holes N and filling ratio $\alpha = (1-\beta)$ via the analytical expressions given by equations (21)–(24) respectively. Simulation have been made for a perforation with one hole per section ($N = 1$) with β change from 0 to 0.95 and for a range of N between 1 and 10 to investigate the effect of the number of holes on the resonance frequency for various values of magnetic field intensity H.

Fig. 2 describes the variation of frequency $f_1 = (\omega_1/2\pi)$ as a function of β with magnetic field effects excluding and including thermal loads and small scale effects. The influence of magnetic field on the change in frequency is clearly visible compared with the frequency of full beam ($\beta = 0$) over a range of β in both cases of EBM and TBM models. Moreover, it is observed that the thermal loads and the small scale effects reduce the value of resonance frequency as mentioned in Refs. [35,38]. Also, the effects of magnetic field is more significant for $H = 6.10^6$ A/m, this is due to the importance of the bending moment effect which is induced by axial magnetic force and varies proportionally with the term ($EI_{eq}/\rho A_{eq}$) and magnetic field intensity [39]. These results confirm those presented in the work of Bourouina et al. [25], *Luschi* and *Pieri* [29] for a clamped-clamped perforated microbeam.

As can be shown in Fig. 2(a), the frequency obtained from EBM model increases by increasing the value of β with and without thermal loads and small scale effects. However, the increasing of magnetic field ($H = 6.10^6$ A/m) which may allow that the fundamental frequency decreases at a point equal to ($\beta = 0.88$) *in* Fig. 2(b), in both the curves of EBM and TBM models can not be intersected. This is due to the importance of the bending moment effect which is induced by axial magnetic force and varies proportionally with the term ($EI_{eq}/\rho A_{eq}$) [39]. The obtained results reveal that the thermal load and the longitudinal magnetic field tend to reduce the nanobeam's flexural stiffness. It is therefore shown that the frequencies would decrease with increasing magnetic field intensity. Indeed, a calculation of fundamental frequency for different magnetic field values is illustrated in Table 1, it is observed that, the frequency calculated from TBM model decreases over the whole range of β and this impact became more significant with the increasing of magnetic field intensity. The divergence in value between the frequencies obtained from EBM and TBM models increases with the hole size ratio β as can be seen in Table 1.

Table 1
Calculation of fundamental frequency for different values of magnetic field intensity, one hole per section ($N = 1$) and varying value of the hole size ratio β.

H (A/m)	2.10^6		4.10^6		6.10^6	
Model β	EBM	TBM	EBM f (GHz)	TBM	EBM	TBM
0	1.8578	1.8137	1.8137	1.7685	1.7378	1.6906
0.2	1.8761	1.8079	1.8306	1.7606	1.7522	1.6790
0.4	1.9414	1.8215	1.8911	1.7678	1.8042	1.6745
0.6	2.0664	1.8188	2.0043	1.7479	1.8963	1.6229
0.8	2.2606	1.6345	2.1589	1.4907	1.9778	1.2137
0.9	2.3761	1.2569	2.1896	0.8534	1.8371	0.8313

As can be shown in Fig. 3, the fundamental frequency evolution as a function of the number of holes N, excluding and including thermal loads and small scale effects. The magnetic field intensity applied in Fig. 3(a) are $H = 4.10^6$ A/m and $H = 4.2.10^6$ A/m in Fig. 3(b) for large hole size ratio $\beta = 0.9$ ($\alpha = 0.1$) [29]. The frequency calculated for both of EBM and TBM models was found to decrease with increasing the number of holes N, this is due to the decrease in the terms ($EI_{eq}/\rho A_{eq}$) and ($EI_{eq}.\rho A_{eq}/kAG_{eq}$) in both respectively. However, for the EBM model, when the number of holes is more than two per section ($N > 2$), the frequency becomes lower than the frequency matching to a full beam ($\beta = 0$), this observation is more considerable for TBM model, the frequency becomes close to zero. Therefore, we can deduce that for larger numbers of holes, the bending moment effect becomes lower than of the bending moment effect matching to a full beam. Indeed, the influence of magnetic field intensity is clearly noticed when $H = 4.2.10^6$ A/m.

In order to show clearly, the influence of the magnetic field

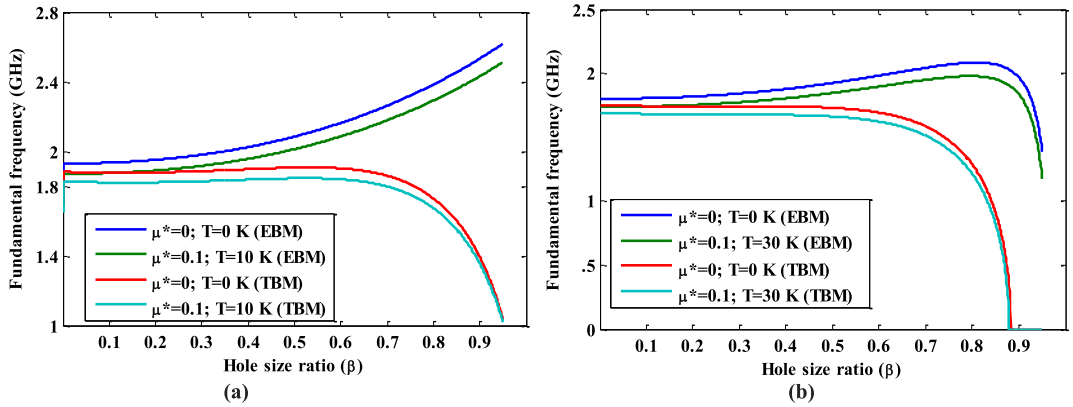

Fig. 2. The fundamental frequency as a function of the hole size ration β for one holes per section ($N = 1$), *(a):* magnetic field intensity $H = 6.10^5$ A/m and *(b):* $H = 6.10^6$ A/m.

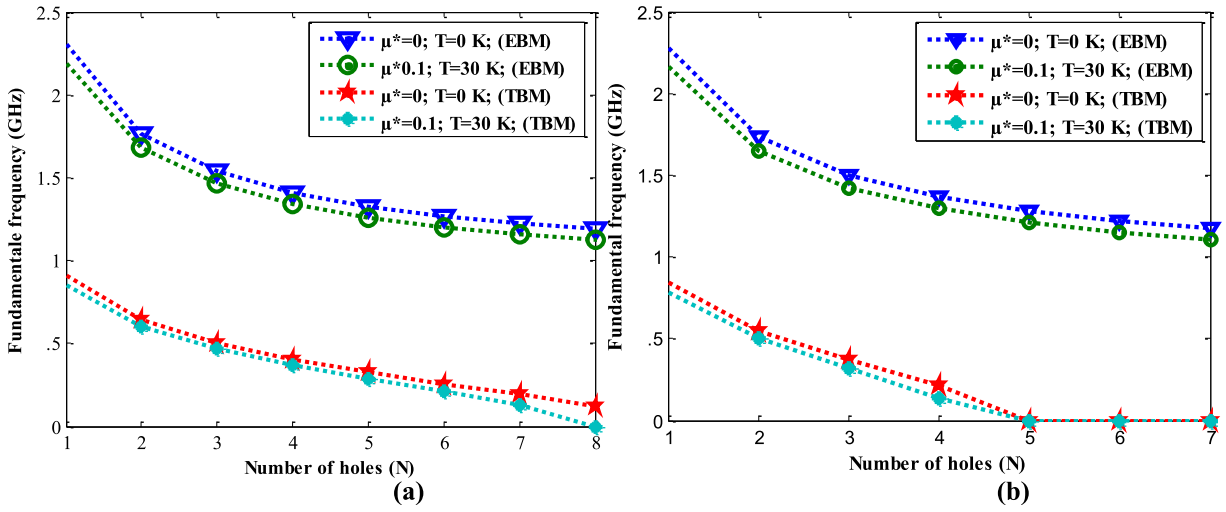

Fig. 3. The fundamental frequency as a function of number of holes N ($\beta = 0.9$) for magnetic field intensity. *(a):* $H = 4.10^6$ A/m and *(b):*$H = 4.2.10^6$ A/m.

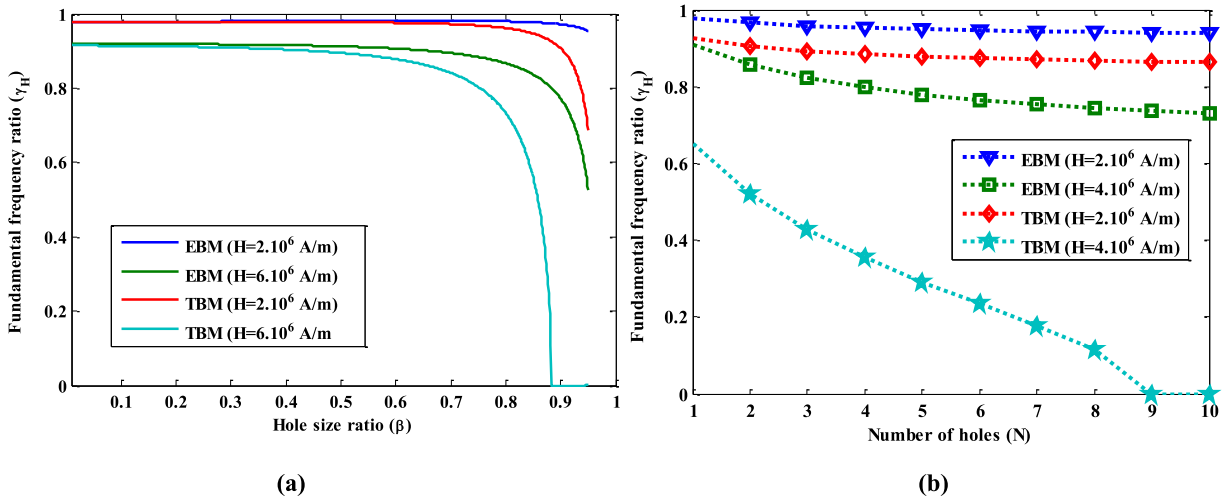

Fig. 4. Magnetic field effect on the fundamental frequency ratio γ_H *(a):* as a function of the hole size ratio β; ($N = 1$ and $\mu^* = 0$ and T = 0); *(b):* as a function of number of holes N; ($\beta = 0.9$, $\mu^* = 0$ and T = 0).

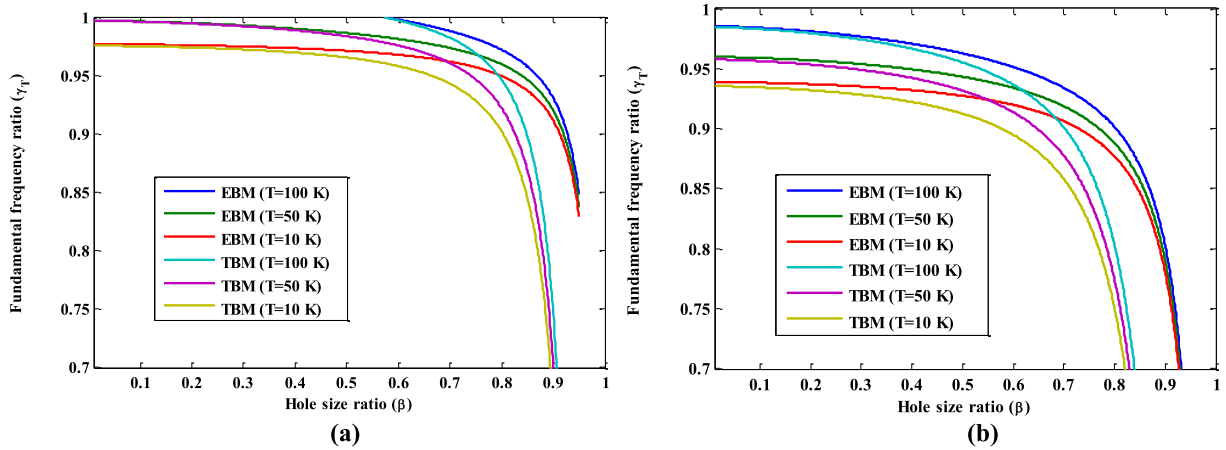

Fig. 5. Thermal loads effect on the fundamental frequency ratio γ_T as a function of the hole size ratio β; ($N = 1$ and $\mu^* = 0$) for magnetic field intensity (a): $H = 4.10^6$ A/m; (b): $H = 6.10^6$ A/m.

intensity, small scale parameter and thermal loads effects on dynamic behavior of perforated nanobeam, results with and without these effects are included. It is very convenient to introduce the ratios of the frequencies with magnetic field, which is a new term in this work, temperature variation and nonlocal parameter to those without magnetic field, temperature variation and nonlocal parameter are respectively given by:

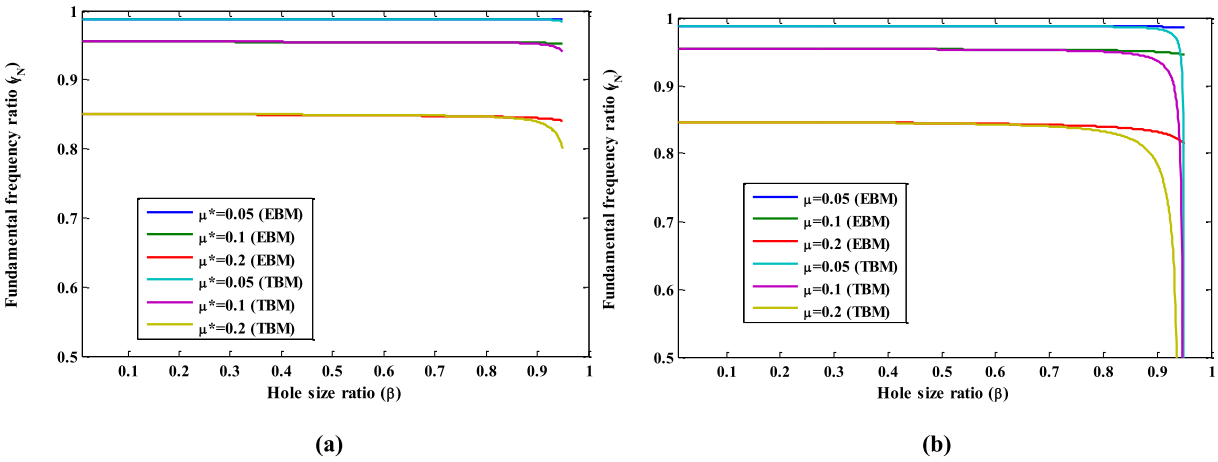

Fig. 6. Small scale effect on the fundamental frequency ratio γ_N as a function of the hole size ratio β; ($N = 1$, $T = 0$ K) for magnetic field intensity (a): $H = 1.5.10^6$ A/m; $H = 2.9.10^6$ A/m).

$$\gamma_H = \frac{(\omega_n)_{LH}}{(\omega_n)_{LO}} \quad \gamma_T = \frac{(\omega_n)_{LT}}{(\omega_n)_{L0}} \quad \gamma_N = \frac{(\omega_n)_{NO}}{(\omega_n)_{L0}} \tag{34}$$

Where $(\omega_n)_{LH}$ is the frequency of the local model including the magnetic field effect, $(\omega_n)_{LT}$ is the frequency of the local model including the thermal loads effect and $(\omega_n)_{NO}$ is the frequency of the nonlocal model when $T = 0$. In order to analyze these effects separately and precisely, a calculation of fundamental frequency ratio is depicted in Figs. 4–6 with detailed discussion.

The dimensionless frequency ratio γ_H is plotted as a function of the hole size ratio β in Fig. 4(a) and as function of number of holes in Fig. 4(b) in both models for various magnetic field values H. It is found that, the ratio γ_H is lower than unity over the whole of β with a decrease by increasing the magnetic field intensity H. This means that the values of frequency which considers the magnetic field effect are lower than those who ignore it. This confirms that the magnetic field effect decrease the resonance frequency of nanobeam as mentioned in Refs. [35,38]. The divergence between the values calculated from EBM and TBM models become reduced with the hole size ratio β and becomes significant at larger values of number of holes (N) due to the importance of shear and rotary effects and the influence of magnetic field intensity.

Now, the dimensionless frequency ratio γ_T is plotted as a function of the hole size ratio β in both models for various Temperature change values T with magnetic field intensity $H = 4.10^6$ A/m in Fig. 5(a) and $H = 6.10^6$ A/m in Fig. 5(b). It is found that, with increasing the temperature change T, the ratio γ_T decreases and is lower than unity over the whole range of β. The divergence between the curves for EBM and TBM models become reduced with the hole size ratio β. This means that the values of magnetic field intensity reduce this effect and the values of frequency which considers the thermal loads effect are lower than those who ignore it. As consequence, the thermal loads effect reduces the resonance frequency of nanobeam as cited in Refs. [35,38].

Fig. 6 illustrates the variation of the fundamental frequency ratio γ_N as a function of β for different values of the nonlocal parameter μ with magnetic field intensity $H = 1.5.10^6$ A/m in Fig. 6(a) and $H = 2.9.10^6$ A/m in Fig. 6(b). It is clear that the dimensionless ratio γ_N is lower than unity over the whole range of β while increasing of nonlocal parameter μ reduces it in the same degree as the fundamental frequencies change. This is due to the bending moment, shear and rotary effects and the influence of magnetic field intensity is more significant for $H = 2.9.10^6$ A/m in Fig. 6(b). In addition, the divergence between the curves of EBM and TBM models tend to be constant for a larger hole size ratio B as indicated in Ref. [35]. Therefore, the small scale effect makes the structure softer and contributes to reduce the resonance frequency that shows the advantage of nonlocal theory to study the dynamic vibration of nanobeam with respect to local theory.

5. Conclusion

In this study, the dynamic vibration of a nanobeam structure composed of a rectangular configuration perforated with periodic square holes network has been analyzed in the framework of Euler–Bernoulli and Timoshenko beam theories including the magnetic field and thermal loads forces. The analytical formulations has been developed to calculate resonance frequency by modifying the dynamics equations and has been used to investigate the magnetic field, small scale and thermal field effects in the presence of a periodic square holes network for both EBM and TBM models. It is found that the resonance frequencies characteristics of this structure are influenced by various parameters such as hole size ratio β with one hole $(N = 1)$ per section, and number of holes for large hole size ratio β, whereas resonance frequencies are lower than those corresponding for a full nanobeam. Also, numerical results demonstrate that the magnetic field, small scale and thermal load effects make the structure softer and contribute to reduce the resonance frequencies of the nanobeam. As consequence, the resonance frequency under magnetic field and thermal loads effects can be modified geometrically by perforation procedure with high sensitivity for a proper design with respect to the conventional structure, in which the resonance frequency change can be controlled by using various parameters.

Acknowledgment

This work was supported by the Algerian PNR domiciled in FUNDAPL Laboratory, University of Blida (Algeria).

References

[1] N. Satish, S. Narendar, K.B. Raju, Magnetic field and surface elasticity effects on thermal vibration properties of nanoplates, Compos. Struct. 180 (2017) 568–580.
[2] S. Foroutan, A. Haghshenas, M. Hashemian, S.A. Eftekhari, D. Toghraie, Spatial buckling analysis of current-carrying nanowires in the presence of a longitudinal magnetic field accounting for both surface and nonlocal effects, Phys. E Low-dimens. Syst. Nanostruct. 97 (2018) 191–205.
[3] C. Liu, L.L. Ke, Y.S. Wang, J. Yang, S. Kitipornchai, Thermo-electro-mechanical vibration of piezoelectric nanoplates based on the nonlocal theory, Compos. Struct. 106 (2013) 167–174.
[4] R. Ansari, E. Hasrati, R. Gholami, F. Sadeghi, Nonlinear analysis of forced vibration of nonlocal third-order shear deformable beam model of magneto–electro–thermo elastic nanobeams, Compos. B Eng. 83 (2015) 226–241.
[5] H. Bourouina, R. Yahiaoui, R. Kerid, M.E.A. Benamar, F. Brioua, Adsorption-induced nonlocal frequency shift in adatoms-nanobeam system, Phys. B Condens. Matter 520 (2017) 128–138.
[6] C. Juntarasaid, T. Pulngern, S. Chucheepsakul, Bending and buckling of nanowires

including the effects of surface stress and nonlocal elasticity, Phys. E Low-dimens. Syst. Nanostruct. 46 (2012) 68–76.
[7] M.S. Gudiksen, L.J. Lauhon, J. Wang, D.C. Smith, C.M. Lieber, Growth of nanowire superlattice structures for nanoscale photonics and electronics, Nature 415 (6872) (2002) 617–620.
[8] X. Duan, Y. Huang, Y. Cui, J. Wang, C.M. Lieber, Indium phosphide nanowires as building blocks for nanoscale electronic and optoelectronic devices, Nature 409 (6816) (2001) 66.
[9] A.I. Hochbaum, R. Chen, R.D. Delgado, W. Liang, E.C. Garnett, M. Najarian, P. Yang, Enhanced thermoelectric performance of rough silicon nanowires, Nature 451 (7175) (2008) 163–167.
[10] F. Ebrahimi, M.R. Barati, A. Dabbagh, A nonlocal strain gradient theory for wave propagation analysis in temperature-dependent inhomogeneous nanoplates, Int. J. Eng. Sci. 107 (2016) 169–182.
[11] R.S. Ruoff, D. Qian, W.K. Liu, Mechanical properties of carbon nanotubes: theoretical predictions and experimental measurements, Compt. Rendus Phys. 4 (9) (2003) 993–1008.
[12] C.H. Ke, N. Pugno, B. Peng, H.D. Espinosa, Experiments and modeling of carbon nanotube-based NEMS devices, J. Mech. Phys. Solid. 53 (6) (2005) 1314–1333.
[13] A. Patti, R. Barretta, F.M. de Sciarra, G. Mensitieri, C. Menna, P. Russo, Flexural properties of multi-wall carbon nanotube/polypropylene composites: experimental investigation and nonlocal modeling, Compos. Struct. 131 (2015) 282–289.
[14] S. Narendar, S. Gopalakrishnan, Nonlocal scale effects on wave propagation in multi-walled carbon nanotubes, Comput. Mater. Sci. 47 (2) (2009) 526–538.
[15] G.F. Wang, X.Q. Feng, Timoshenko beam model for buckling and vibration of nanowires with surface effects, J. Phys. D Appl. Phys. 42 (15) (2009) 155411.
[16] A.T. Samaei, B. Gheshlaghi, G.F. Wang, Frequency analysis of piezoelectric nanowires with surface effects, Curr. Appl. Phys. 13 (9) (2013) 2098–2102.
[17] V. Atabakhshian, A. Shooshtari, M. Karimi, Electro-thermal vibration of a smart coupled nanobeam system with an internal flow based on nonlocal elasticity theory, Phys. B Condens. Matter 456 (2015) 375–382.
[18] J. Avsec, M. Oblak, Thermal vibrational analysis for simply supported beam and clamped beam, J. Sound Vib. 308 (3) (2007) 514–525.
[19] S.R. Asemi, A. Farajpour, Thermo-electro-mechanical vibration of coupled piezoelectric-nanoplate systems under non-uniform voltage distribution embedded in Pasternak elastic medium, Curr. Appl. Phys. 14 (5) (2014) 814–832.
[20] V. Atabakhshian, A. Shooshtari, M. Karimi, Electro-thermal vibration of a smart coupled nanobeam system with an internal flow based on nonlocal elasticity theory, Phys. B Condens. Matter 456 (2015) 375–382.
[21] F. Ebrahimi, M.R. Barati, On nonlocal characteristics of curved inhomogeneous Euler–Bernoulli nanobeams under different temperature distributions, Appl. Phys. A 122 (10) (2016) 880.
[22] L.L. Ke, Y.S. Wang, Free vibration of size-dependent magneto-electro-elastic nanobeams based on the nonlocal theory, Phys. E Low-dimens. Syst. Nanostruct. 63 (2014) 52–61.
[23] S. Narendar, S. S. Gupta, S. Gopalakrishnan, Wave propagation in single-walled carbon nanotube under longitudinal magnetic field using nonlocal Euler–Bernoulli beam theory. Appl. Math. Model., 36(9), 4529–4538.
[24] F. Ebrahimi, M.R. Barati, Magnetic field effects on buckling behavior of smart size-dependent graded nanoscale beams, Eur. Phys. J. Plus 131 (7) (2016) 1–14.
[25] H. Bourouina, R. Yahiaoui, A. Sahar, M.E. Benamar, Analytical modeling for the determination of nonlocal resonance frequencies of perforated nanobeams subjected to temperature-induced loads, Phys. E Low-dimens. Syst. Nanostruct. 75 (2016) 163–168.
[26] J. Chan, M. Eichenfield, R. Camacho, O. Painter, Optical and mechanical design of a “zipper” photonic crystal optomechanical cavity, Optic Express 17 (5) (2009) 3802–3817.
[27] W.N. Sharpe Jr., R. Vaidyanathan, B. Yuan, G. Bao, R.L. Edwards, Effect of etch holes on the mechanical properties of polysilicon, J. Vac. Sci. Technol. B: Microelectron. Nanometer Struct. Process. Measure. Phenom. 15 (5) (1997) 1599–1603.
[28] V.L. Rabinovich, R.K. Gupta, S.D. Senturia, The effect of release-etch holes on the electromechanical behaviour of MEMS structures, Solid State Sensors and Actuators, 1997. TRANSDUCERS'97 Chicago, 1997 International Conference on, vol. 2, IEEE, 1997, June, pp. 1125–1128.
[29] L. Luschi, F. Pieri, An analytical model for the determination of resonance frequencies of perforated beams, J. Micromech. Microeng. 24 (5) (2014) 055004.
[30] L. Luschi, F. Pieri, An analytical model for the resonance frequency of square perforated Lamé-mode resonators, Sensor. Actuator. B Chem. 222 (2016) 1233–1239.
[31] S. Sahmani, M.M. Aghdam, Nonlocal strain gradient shell model for axial buckling and postbuckling analysis of magneto-electro-elastic composite nanoshells, Compos. B Eng. 132 (2018) 258–274.
[32] A.C. Eringen, Int. J. Eng. Sci. 30 (10) (1992) 1551–1565.
[33] H.L. Lee, W.J. Chang, Jpn. J. Appl. Phys. 48 (6R) (2009) 065005.
[34] S. M. Han, H. Benaroya, T. Wei, 1999; 225(5), 935–988.
[35] A. Benzair, A. Tounsi, A. Besseghier, H. Heireche, N. Moulay, L. Boumia, J. Phys. (Paris) D 41 (22) (2008) 225404.
[36] Y. Zhao, C.C. Ma, G. Chen, Q. Jiang, Phys. Rev. Lett. 91 (17) (2003) 175504.
[37] J.F. Doyle, Static and Dynamic Analysis of Structures: with an Emphasis on Mechanics and Computer Matrix Methods vol. 6, Springer Science & Business Media, 1991, p. 146.
[38] Y.Q. Zhang, X. Liu, G.R. Liu, Nanotechnology 18 (44) (2007) 445701.
[39] S. Kumar, R. Pratap, Sens. Actuators, A 125 (2) (2006) 304–312.
[40] M. Arefi, A.M. Zenkour, Size-dependent free vibration and dynamic analyses of piezo-electro-magnetic sandwich nanoplates resting on viscoelastic foundation, Phys. B Condens. Matter 521 (2017) 188–197.
[41] Y. Yang, C.W. Lim, Non-classical stiffness strengthening size effects for free vibration of a nonlocal nanostructure, Int. J. Mech. Sci. 54 (1) (2012) 57–68.
[42] L.L. Ke, Y.S. Wang, Z.D. Wang, Nonlinear vibration of the piezoelectric nanobeams based on the nonlocal theory, Compos. Struct. 94 (6) (2012) 2038–2047.
[43] J.Q. Zhang, S.W. Yu, X.Q. Feng, J. Phys. D 41 (2008) 125306–125308.
[44] B. Gheshlaghi, S.M. Hasheminejad, Curr. Appl. Phys. 11 (2011) 1035–1041.
[45] D. Karličić, D. Jovanović, P. Kozić, M. Cajić, Thermal and magnetic effects on the vibration of a cracked nanobeam embedded in an elastic medium, J. Mech. Mater. Struct. 10 (1) (2015) 43–62.
[46] H.L. Dai, S. Ceballes, A. Abdelkefi, Y.Z. Hong, L. Wang, Exact modes for post-buckling characteristics of nonlocal nanobeams in a longitudinal magnetic field, Appl. Math. Model. 55 (2018) 758–775.